行政院國家科學委員會專題研究計畫期末成果報告

仿生型自主式水下載具行為控制系統之研究(III)

Study on the Behavior Control System of Biomimetic AUVs(III)

計畫編號：NSC 90-2611-E-002-030

執行期限：90 年 8 月 1 日至 91 年 7 月 31 日

主持人：郭振華

國立臺灣大學造船及海洋工程學系

Abstract – The report presents a biomimetic autonomous underwater vehicle (BAUV) that mimics the shape and behavior of fishes. The swimming motion of the BAUV is achieved by an oscillating foil. We parameterize the body spline by a set of parameters. Then we optimized the parameter set using Genetic Algorithms (GAs) by evaluating a fitness function through many swimming trials in a water tank. The fitness function of the optimization is defined as the ratio of the forward velocity to the required driving power of joint motors. It is found that the resulting body spline is the best compared to all other body splines among all tail-beating frequencies. And there is an optimal tail-beating frequency for one particular body spline.

Index Terms – Underwater Vehicle, Biomimetic, GAs

摘要

現階段自主式水下載具基本架構乃軍用潛艦或魚雷之架構與自動控制技術之單純組合，並未由自主性及運用目的之觀點進行感測器、訊號處理器、運動控制器、致動器、推進器及外型之整合最佳化，致存在諸如小範圍運動之靈活性不足、推進效率偏低、無法適應未知作業環境等問題。仿生型水下載具是藉由身體擺動的方式游泳推進，如何控制載具以最佳的擺動模式游泳是本文研究的目標。魚在游泳時身體與流體之間的作用力模式十分複雜，因此我們藉由以游泳模式運動的載具，經由實驗探討其最佳的擺動模式。首先，我們將魚的脊椎曲線參數化，然後藉由載具游泳試驗量取的數據計算其評價函數後，經基因演算法將參數最佳化。而此評價函數定義為載具游泳的輸出功率比上驅動馬達的輸入功率。文中同時藉由模擬與實驗進行參數最佳化，並探討游泳機構的設計問題，如齒輪比、仿生型載具的最大前進速度等。

關鍵詞：水下載具、水下導航、水下技術

I. Introduction

Recently, the combination of engineering and biology has become a new direction of science and technology. A fishlike Autonomous Underwater Vehicle (AUV) testbed named BAUV is under developing in National Taiwan University to investigate interactions and coordination among appearance, motion, behavior, and perception. In this report, we derive an optimal swimming pattern for the BAUV testbed by evaluating the ratio of forward velocity to the driving power of joint motors. To find an optimal swimming pattern, we need to find the best traveling body spline for the vehicle. Besides, we have to develop a program for motion control to manipulate joint motors for performing the desired traveling body spline. The results are fundamental for our researches such as propulsive efficiency measurements, guidance, and control of the BAUV testbed.

The overview of fish swimming modes for aquatic locomotion was presented in [1]. Fish swim either by body and/or caudal fin (BCF) movements or using median and/or paired fins (MPF) propulsion. Basing on the type of movements (oscillatory or undulatory) employed for thrust generation, specific swimming modes are identified for both BCF and MPF locomotion. Chiu el al. [2] did simulation on undulatory locomotion of a flexible slender body. Chiu et al. [3] analyzed the dynamic characteristics of a BAUV. Guo et al. [4] presented a method to coordinate body segments and paired fins for the BAUV motion control. Barrett et al. [5] used GAs to evolve the optimal fish body motion for 'RoboTuna'. Many methods for the measurement of the power of swimming fish are developed, for example [6][7]. Wardle and Reid [8] experimented to measure the power output of large cod with the large amplitude elongated body theory by Lighthill. Moreover, the study to investigate the mechanical control of speed in steady undulatory swimming had been presented in [9].

The report is organized as follows: Section II explains how we define the body spline and find the optimal body spline by evaluating the ratio of the swim speed to the required driving motor power. The descriptions of the experimental procedure and the results are presented in Sectoin III. Finally, concluding remarks are provided in Section IV.

II Fitness function

We define three coordinate systems: space-fixed coordinate system $O-XY$, body-fixed coordinate system $o-xy$ (global) and segment-fixed coordinate system $\tilde{o}_i-\tilde{x}_i\tilde{y}_i$ (local) as shown in Figure 1. Each coordinate can be transferred to another one by using the relationship of the position and angle between two coordinate systems.

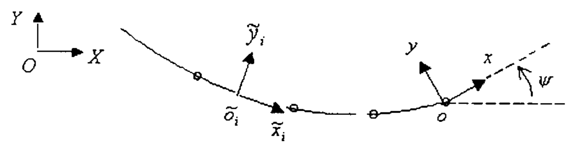

Fig. 1 Definition of coordinate systems

From observations of biological fishes [10][11], the body spline motion can be considered as traveling waves that increase in amplitude from the nose to the tail. A specific form of traveling wave equation which is a slight derivation from that originally suggested by Lighthill [12] was developed. Let the body spline take the form of a traveling wave given by

$$y(x,t) = y_1(x)\sin(kx + \omega t)\cdot(1 - e^{-\frac{t}{T_d}}) \qquad (1)$$

where

y : transverse displacement of body

$y_1(x)$: the amplitude envelope; here we define $y_1(x) = c_1 x + c_2 x^2$

x : displacement along the main axis

$k = 2\pi / \lambda$; body wave number

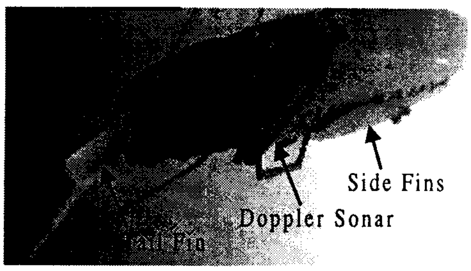

Fig. 2 Photograph of the testbed vehicle in a water tank

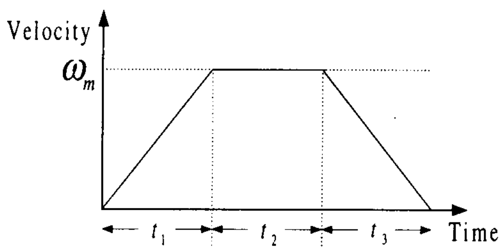

Figure 3 Motor velocity profile

λ : body wave length

c_1 : coefficient of linear wave amplitude envelope

c_2 : coefficient of quadratic wave amplitude envelope

$\omega = 2\pi f = 2\pi / T$; body wave frequency

T : body wave period

T_d : period of the initial undulating delay cycle

Eq (1) expresses a sinusoidal wave traveling from nose to tail (i.e. from $x = 0$ to $x = -L$) within the bounds of a second-order ($c_1 x + c_2 x^2$) amplitude envelope. The exponential term defining the initial delay when the body starts to undulate is for the convergence of numerical calculation. The slope of the body is $y_x(x,t) \equiv \partial y / \partial x$, the angle between the body and the x-axis is $\theta \equiv \tan^{-1} y_x$.

To obtain a highly efficient mode for swimming, we define a fitness function as

$$Fitness\ Function = \frac{Forward\ Swimming\ Velocity}{Motor\ \ Power\ \ Input} \qquad (2)$$

The fitness function represents the transmission efficiency of the drive system. The reason we did not set the fitness function as the ratio of the swimming power output to the motor power input is that swimming power output provides not only the power to move forward but also the power to move laterally. Besides, the forward swimming velocity of the vehicle is diretly measurable.

Motor power dissipation can be discussed in the case of incremental motion where the motor steps periodically following a trapezoidal velocity profile, as shown in Figure 3. The motor accelerates over t_1 to the velocity ω_m and runs at that speed for t_2. Later, it decelerates to zero velocity over t_3.

The analysis of determining the average power loss in the motor can be found using Eq (3) [13]. The average power dissipation $\overline{P}$ was found to have five terms.

$$\overline{P} = P_1 + P_2 + P_3 + P_4 + P_5$$

$$\begin{aligned}
P_1 &= \frac{fRJ^2\omega_m^2}{K_T^2}\left(\frac{1}{t_1} + \frac{1}{t_3}\right) \\
P_2 &= \frac{fR}{K_T^2}\left(T_f + T_L + D\omega_m\right)^2 t_2 \qquad (3) \\
P_3 &= \frac{fR}{K_T^2}\left[\left(T_f + T_L\right)^2 + \left(T_f + T_L\right)D\omega_m + \frac{1}{3}D^2\omega_m^2\right](t_1 + t_3) \\
P_4 &= \frac{fK_E T_f \omega_m}{2K_T}(t_1 + 2t_2 + t_3) \\
P_5 &= \frac{fK_E D\omega_m^2}{3K_T}(t_1 + 3t_2 + t_3)
\end{aligned}$$

where:

K_T : torque constant

K_E : voltage constant

R : resistance

T_f : friction constant

D : viscous damping

T_L : load torque

f : frequency

$J = J_m + J_L$ (total moment inertia) = (motor) + (load)

The various terms can be interpreted physically. P_1

describes the power dissipation due to the acceleration and deceleration of the motor and load. P_2 and P_3 describe the winding losses due to the opposing torques during the various intervals of motion. Finally, P_4 and P_5 represent the rotational losses due to the constant torque T_f and the damping D respectively. Table 1 shows the motor parameters we are using for our testbed.

To calculate the load torque T_L, we need to make assumptions on the hydrodynamic model. The fluid interaction forces composed of friction C_f and cross flow drag C_d can be written as:

Table 1 Motor parameters

Parameters \Motor	BSM80A-250AE (body joint)	BSM50A-233ME (tail joint)
K_T (Nm/amp)	0.55	0.38
K_E $(V/rad\cdot s^{-1})$	0.3228	0.2187
R (Ω)	1.8	4.07
T_f (Nm)	$4.24\cdot10^{-2}$	$4.24\cdot10^{-2}$
D $(Nm/rad\cdot s^{-1})$	$2.7\cdot10^{-4}$	$2.7\cdot10^{-4}$
J_m (kgm^2)	$1.72\cdot10^{-4}$	$1.3\cdot10^{-5}$

$$\begin{cases} F_{\tilde{x}_i} = -m_{xi}\dot{\tilde{u}}_i + m_{y_i}\tilde{v}_i\dot{\tilde{\psi}}_i - \frac{1}{2}\rho\,\tilde{u}_i|\tilde{u}_i|\cdot C_f\cdot S_i \\ F_{\tilde{y}_i} = -m_{y_i}\dot{\tilde{v}}_i - m_{xi}\tilde{u}_i\dot{\tilde{\psi}}_i - \frac{1}{2}\rho\,\tilde{v}_i|\tilde{v}_i|\cdot C_d\cdot d_i\cdot\Delta L \\ G_{\tilde{z}_i} = -J_{zi}\ddot{\tilde{\psi}}_i - (m_{y_i}-m_{xi})\tilde{u}_i\tilde{v}_i - \rho\dot{\tilde{\psi}}_i|\dot{\tilde{\psi}}_i|\cdot C_d\cdot d_i\cdot\frac{(\Delta L)^4}{64} \end{cases} \tag{4}$$

Here, the forces are acting on the i^{th} segment described in the segment-fixed coordinate $\tilde{o}_i - \tilde{x}_i\tilde{y}_i$,

and

$m_i, m_{xi}, m_{yi}, J_{zi}$: the mass, added masses in the $\tilde{x}_i, \tilde{y}_i, \tilde{z}_i$, respectively;

C_f : friction coefficient;

C_d : sectional cross flow drag coefficient;

S_i : the wet surface area of the i^{th} segment;

d_i : the height of the cross-section of the i^{th} segment (perpendicular to the y-axis);

ρ : fluid density

ΔL : segment length

We then translate it to space-fixed coordinate by

$$\begin{bmatrix} F_{x_i} \\ F_{y_i} \end{bmatrix} = \begin{bmatrix} \cos\psi_i & -\sin\psi_i \\ \sin\psi_i & \cos\psi_i \end{bmatrix} \begin{bmatrix} F_{\tilde{x}_i} \\ F_{\tilde{y}_i} \end{bmatrix} \tag{5}$$

So the total torque τ that motor need to resist due to the fluid interaction forces are

$$\tau = \sum_{i=mp}^{n} \tau_i + \sum_{i=mp}^{n}\left(F_{y_i}\bar{x}_i - F_{x_i}\bar{y}_i\right) \tag{6}$$

In Eq (3), the load moment inertia J_L is calculated by

$$J_L = \sum_{i=mp}^{n} J_{zi} \tag{7}$$

where

mp : joint position

n: number of segments

We define a GAs'chromosome for the body spline as $\{ c_1, c_2, \lambda, T \}$. Every parameter has four genes, and each gene is a decimal integer (0~9). In other words, the whole chromosome has 16 bits such as {0053003338528063}. For example, the above chromosome represents c_1 =-0.053, c_2 =0.033, λ =3.852, T =8.063 respectively. The optimization procedure using the GAs includes three transformation operators, reproduction, crossover, and mutation.

III. Experiments

The BAUV is segmented to five components: head, tail, tail fin, and two pectoral fins. The head segment and the tail fin are rigid, and the tail part is supported using by a rigid link. There are six brushless DC servo motors mounted inside the BAUV. The Doppler sonar is set in the abdominal part of the BAUV for sensing the direction, velocity, and water depth. Only two motors located on the body spline are powered in our experiments.

The flow chart of the optimization procedure is shown in Figure 4. To reduce computational time, the control parameter T is fixed at 4 sec during the optimization procedure. Evolutions were carried out to the tenth generation. The initial and the resulting parameter values are shown in Table 2 and 3. Fitness variations vs. time for the full process of evolution appears in Figure 5.

Four chromosomes of different oscillation amplitudes were chosen as follows,

Chromosome1: { c_1 =-0.0750, c_2 =0.0170, λ =3.522 }
Chromosome2: { c_1 =-0.0750, c_2 =0.0260, λ =3.622 }
Chromosome3: { c_1 =-0.0520, c_2 =0.0110, λ =3.522 }
Chromosome4: { c_1 =-0.0940, c_2 =0.0207, λ =6.510 }

Among them, Chromosome1 is the optimal one from experiment results. Chromosome4 is the optimal one from simulation results using the simulation software presented in [2] [3]. Every parameter set was experimented with period T =3, 3.5, 4, 4.5, 5, 5.5, and 6 sec.

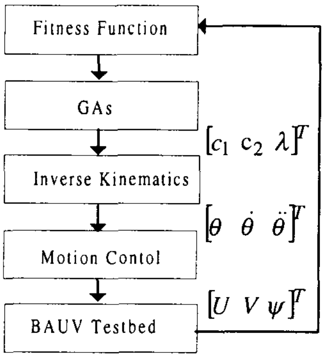

Fig. 4 The closed-loop optimization procedure

Table 2 Initial population
Mean Fitness = 1.07%, Max Fitness = 1.46%

Test#	c_1	c_2	λ (m)	T (sec)	Fitness
1	-0.0940	0.0160	3.2220	4	0.0146
2	-0.0750	0.0040	4.6890	4	0.0121
3	-0.0330	0.0230	5.9160	4	0.0092
4	-0.0120	0.0500	3.5770	4	0.0043
5	-0.0940	0.0410	6.3900	4	0.0116
6	-0.0030	0.1230	5.5740	4	0.0084
7	-0.0320	0.0850	6.8280	4	0.0110
8	-0.0240	0.1060	5.8510	4	0.0106
9	-0.0230	0.0360	5.8990	4	0.0142
10	-0.0200	0.0760	5.1520	4	0.0110

Table 3 Tenth generation
Mean Fitness = 1.55%, Max Fitness = 1.78%

Test#	c_1	c_2	λ (m)	T (sec)	Fitness
1	-0.0750	0.0170	3.5220	4	0.0178
2	-0.0760	0.0170	3.5220	4	0.0145
3	-0.0750	0.0170	3.5220	4	0.0178
4	-0.0750	0.0130	3.5620	4	0.0149
5	-0.0750	0.0170	3.5220	4	0.0178
6	-0.0750	0.0170	3.5220	4	0.0178
7	-0.0750	0.0360	3.5220	4	0.0122
8	-0.0750	0.0170	4.5220	4	0.0126
9	-0.0750	0.0170	3.5280	4	0.0149
10	-0.0750	0.0130	3.5620	4	0.0149

Figure 6 shows the relation between Fitness function and the forward velocity using the body splines parameterized with different chromosomes. The Fitness function values generated from the optimal chromosome at different forward velocities is always higher than others. Figure 7 illustrates the frequency ($2\pi/T$) dependence of forward velocity at different amplitudes of the caudal fin. It is shown that higher oscillation frequency and larger amplitude generates larger forward velocity. Figure 8 illustrates the period T dependence of the yaw, roll, pitch motions at the optimal condition. Figure 9 illustrates the sway motion vs. the period T. The amplitude of sway decreases with T. Yaw and pitch angle as well as the roll angle rise up slowly when the period decreases.

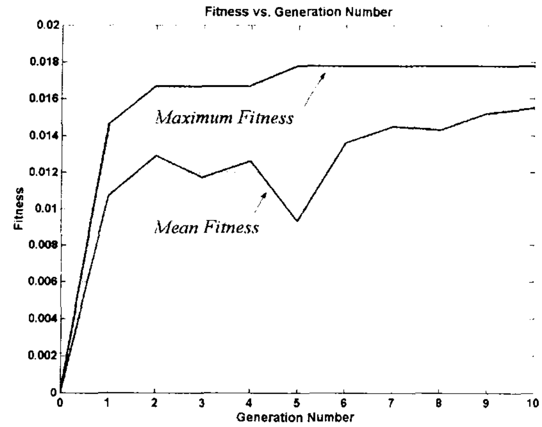

Fig. 5 Graph of generational *Fitness Function*

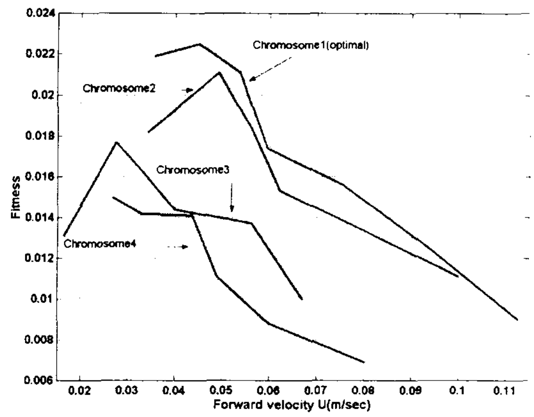

Fig. 6 Forward velocity vs. *Fitness Function* of four body splines

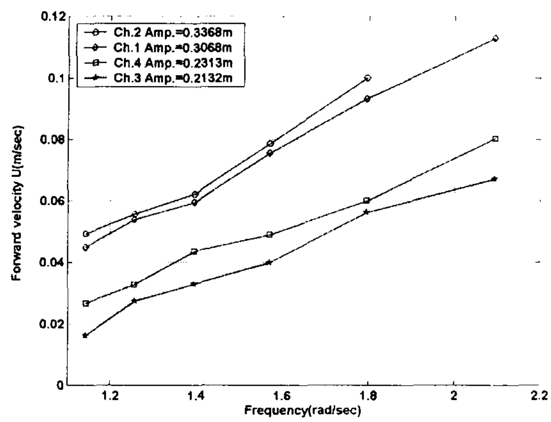

Fig. 7 Frequency vs. forward velocity at different amplitudes

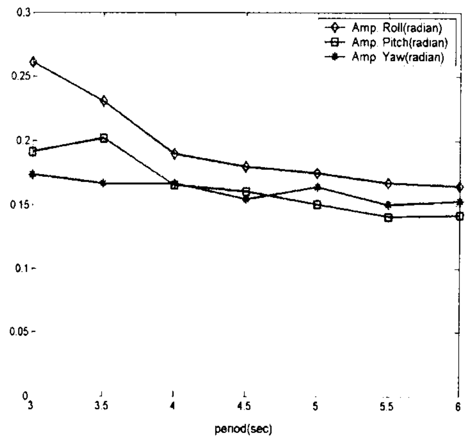

Fig. 8 Motions vs. body wave period

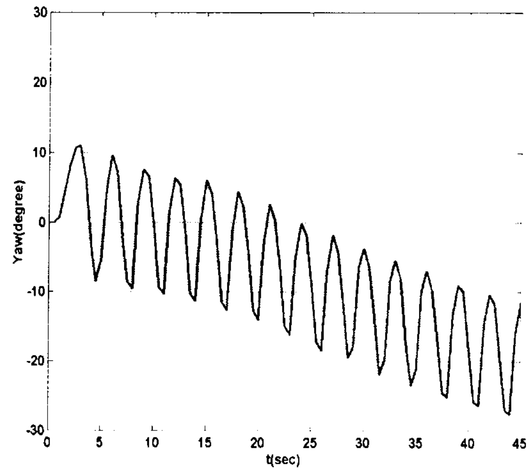

Fig. 11 Time history of the yaw angle

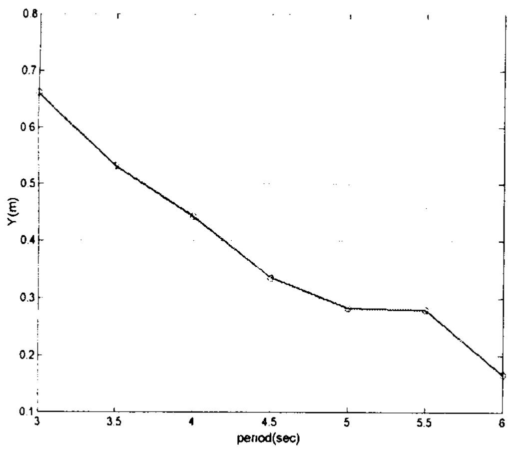

Fig. 9 Sway motion vs. body wave period

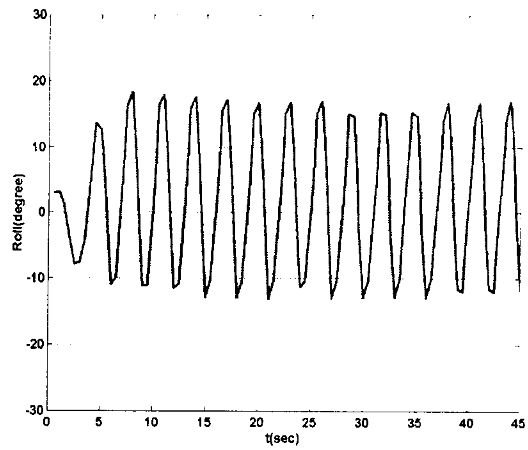

Fig. 12 Time history of the roll angle

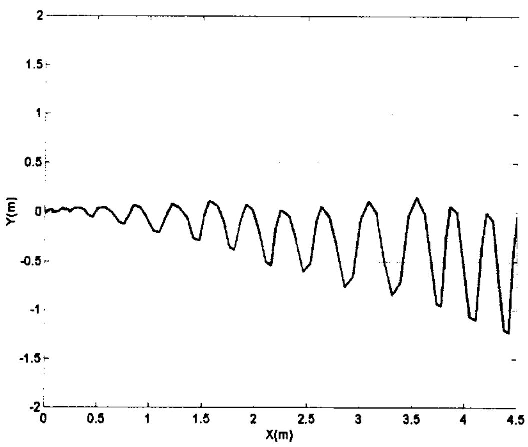

Fig. 10 Trajectory of the BAUV's head

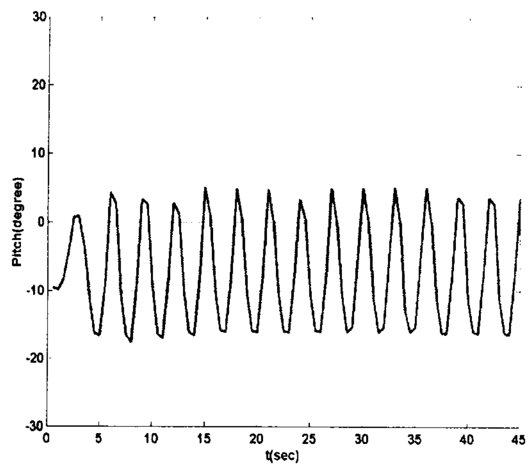

Fig. 13 Time history of the pitch angle

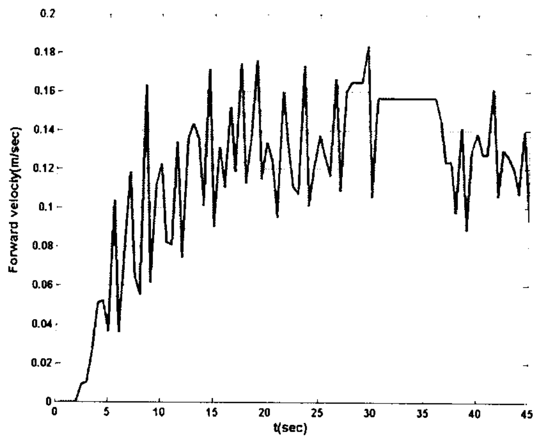

Fig. 14 Time history of the forward velocity

From our data, the swimming of the BAUV causes considerable roll, pitch and larger yaw motion. These noticeable roll and pitch motions cause more power losses, and consequently the BAUV swims more slowly. Figures 10 to 14 represent the typical data from the experiments. They are records from the swimming using the body spline derived from the optimal chromosome: $\{c_1=-0.075, c_2=0.017, \lambda=3.522\}$ including trajectory and time histories of yaw, roll, pitch angle as well as forward velocity. In these figures, $T=3$ sec.

IV. Concluding Remarks

In this report, we applied the Genetic Algorithms to evolve the optimal traveling body spline for the drive system of a biomimetic AUV. The fitness function of the optimization is defined as the ratio of the swim velocity to the required driving motor power. The optimization is carried out by experiments in a water tank. The constraints of motor speed and torque are considered in our formulation to avoid excessive command signals.

We have demonstrated by experiments that we can improve the motor efficiency by selecting the optimal body spline motion of the BAUV. The optimal swimming pattern at a fixed forward velocity is optimal for all forward velocities.

Large pitch and roll motions are observed in the experiments. To reduce these recoil motions, further considerations in the shape design and the use of stabilizing fins are needed.

How to improve the motor efficiency by selecting proper gear ratios of joint motors will be one of our further research subjects. The elastic tissues in cetaceans have the properties of saving swimming energy. Consequently, it is better in the future to include the influence of elastic materials set in the caudal region of the BAUV. To improve the maneuverability of a BAUV, we need to include the hydrodynamic model of pectoral fin motion in our control system modelin the future. Besides, to mimic biological fishes, we could apply some advanced control methods to develop more complex swimming behavior.

References

[1] Michael Sfakiotakis, David M. Lane, and J. Bruce C. Davies, "Review of fish swimming modes for aquatic locomotion," *IEEE Journal of Oceanic Engineering* Vol.24. No 2, April 1999.

[2] F.C. Chiu, C.P. Wu, J. Guo, "Simulation on the Undulatory Locomotion of a Flexible Slender Body," *1st Int'l Symp. on Aqua Bio-Mechanisms*, Hawaii, U.S.A., 2000.

[3] Forng-Chen Chiu, Jenhwa Guo, Ji-Gang Chen, Yen-Hwa Lin, "Dynamic characteristic of a biomimetic underwater vehicle," *Proc. of the IEEE Symp. On Underwater Technology*, Tokyo, Japan, pp. 172-177, 2002.

[4] J. Guo, F. C. Chiu, S. W. Cheng, Y. J. Joeng, " Motion control and way-point tracking of a biomimetic underwater vehicle," *Proc. of the IEEE Symp. On Underwater Technology*, Tokyo, Japan, pp. 73-78, 2002.

[5] D. Barrett, M. Grosenbaugh, M. Triantafyllou, "The optimal control of a flexible hull robotic undersea vehicle propelled by an oscillating foil," *Porc. Of the IEEE Symp. On Autonomous Underwater Technology*, Monterey, CA, pp. 1-9, 1996.

[6] Karen A. Harper, Matthew D. Berkemeier, and Sheryl Grace, "Modeling the dynamics of spring-driven oscillating-foil propulsion," *IEEE Journal of Oceanic Engineering*, Vol. 23, No. 3, July 1998.

[7] Reinhard Blickhan and Jian-Yu Cheng, "Energy storage by elastic mechanisms in the tail of large swimmers—a re-evaluation," *J. Theor. Biol.*, 168, 315-321, 1994.

[8] C. S. Wardle and A. Reid, "The application of large amplitude elongated body theory to measure swimming power in fish," *Fisheries Mathematics*, edited by J. H. Steele, Academic Press, London, 1977.

[9] Matthew J. Mchency, Charles A. Pell and John H. Long Jr., "Mechanical control of swimming speed: stiffness and axial wave form in undulating fish models," *The Journal of Experimental Biology*, 198, 2293-2305, 1995.

[10] J. J. Viedler and F. Hess, "Fast continuous swimming of two pelagic predators, Saithe and Mackel: a kinematic analysis," *Journal of Experimental Biology*, 109, pp.209-228, 1984.

[11] H. Dewar, *Studies of tropical tuna swimming performance: thermoregulation, swimming mechanics and energetics*, PhD Thesis in Marine Biology, University of California, San Diego, 1993.

[12] M. J. Lighthill, "Note on the swimming of slender fish," *J. Fluid Mech.*, vol. 9, pp.305-317, 1960.

[13] Electro-Craft, *DC servo motors, speed control, servo systems*, Electro-Craft Corp., Minnesota, U.S.A.